

## Research Article

# Assessment of Mechanical Performance and Quality Assurance in Fabricated AA6061-T6

Anesti Nasi<sup>1</sup>, Kledi Ushe<sup>1</sup>, Klodian Dhoska<sup>1,\*</sup>, Anis Sulejmani<sup>1</sup>, Odhisea Koça<sup>1</sup>, Panagiotis Kyratsis<sup>2</sup>, Aleksandra Petrovic<sup>3</sup>

<sup>1</sup> Department of Mechanics, Polytechnic University of Tirana, Tirana, Albania.

<sup>2</sup> Department of Product and Systems Design Engineering, University of Western Macedonia, Kozani, Greece.

<sup>3</sup> Department of Traffic Engineering, University of Pristina Kosovska Mitrovica, Mitrovica, Serbia.

## ARTICLE INFO

### Article History

Received 17 Jan 2026  
Revised 15 Feb 2026  
Accepted 12 Mar 2026  
Published 13 Apr 2026

### Keywords

Measurement  
Uncertainty,  
Tensile Strength,  
Aluminum Alloy,  
Quality Control,  
Mechanical  
Characterization.



## ABSTRACT

This paper focuses on integrated methodology for the experimental mechanical properties of produced AA6061 aluminum alloy, coupled for a rigorous quality assurance framework to validate material reliability for structural applications. The approach combines microstructural analysis, tensile testing analysis, and systematic measurement uncertainty quantification, all performed through the relevant international standards. To ensure statistical reliability, the overall standard uncertainty was computed utilizing the propagation law of uncertainty for  $k = 2$  with a confidence level of roughly 95%. The experimental results yielded a tensile strength of  $309.4 \pm 4.0 \text{ N/mm}^2$ , showing excellent repeatability with a lower relative uncertainty that correspond to 1.3%. These values not only meet the mechanical property requirements stipulated in international standards for AA6061 alloy but also confirm the experimental protocol reliability. The findings validate the material's suitability for demanding engineering environments and highlight the importance of embedding uncertainty quantification within standard characterization practices to support informed design decisions.

## 1. INTRODUCTION

During the last decade, aluminum alloys have become essential to contemporary mechanical engineering, valued for their high strength-to-weight ratio, corrosion resistance, low density, and adaptability to diverse production processes [1-3]. These properties make them ideal for structural and load-bearing applications across aerospace, automotive, transportation, and energy industries, where lightweight design is critical [4-6].

The Al-Mg-Si series, in particular, offers an excellent balance of ductility, strength, and ease of fabrication. Among these, AA6061 is the most widely used heat-treatable alloy, usually employed in structural frames, machine parts, pressure vessels, and welded assemblies [7]. Through T6 heat treatment procedure it has been enhanced the mechanical properties of the AA6061, which boosts yield and tensile strength without compromising ductility and toughness [8]. Furthermore, AA6061 offers good machinability and weldability, which have been used in many complex components manufactured by extrusion, forging, and machining [3, 19, 10].

A critical challenge in engineering design is that the actual mechanical behavior of AA6061 components can diverge from the standardized values listed in international specifications. This divergence is primarily caused by manufacturing variables. Factors such as the uniformity of cooling rates prior thermomechanical processing, chemical composition tolerances, heat treatment, and residual stress all have a direct influence on the alloy's microstructure and its resulting mechanical properties [10]. Consequently, variations in elastic modulus, yield strength, tensile strength, and ductility are common, with direct consequences for structural performance and the safety margins of a design.

To mitigate this uncertainty, it is essential to characterize the material as manufactured. Experimental tensile testing provides a direct method for capturing the true stress-strain response and deriving the mechanical parameters that are needed for reliable structural analysis accompanied with numerical modeling [11]. The importance of this direct approach is further

\*Corresponding author. Email: [kdhoska@fim.edu.al](mailto:kdhoska@fim.edu.al).

underscored by the inherent variability in all experimental work, which can be introduced by material heterogeneity, specimen preparation, or testing conditions, and must be accounted for to ensure data credibility.

Mechanical properties derived from tests are not fixed values but are subject to inherent uncertainty. Quantifying this uncertainty has become critical in modern mechanical engineering, underpinning reliability-based design and performance assessment [11-16]. Measurement uncertainty directly affects the determination of material properties, which in turn impacts failure analyses, fatigue life predictions, and finite element simulations. Ignoring it can lead to designs that are either needlessly conservative or unsafely optimistic [17-19]. Integrating uncertainty analysis into mechanical characterization is therefore essential for producing credible, robust data that supports sound engineering decisions.

Adopting this framework, the current study provides a thorough mechanical characterization of manufactured AA6061 aluminum alloy. It focuses on tensile behavior and key mechanical parameters, while simultaneously conducting an uncertainty assessment to establish the reliability and confidence levels of the results. Through this integrated approach, the research aims to deliver dependable material data for use in advanced modeling, structural integrity assessments, and the optimized design of components utilizing AA6061 aluminum alloy.

This work presents a novel integration of experimental mechanical characterization and systematic uncertainty quantification for manufactured AA6061 aluminum alloy. Its purpose is to move beyond simple property reporting by providing the confidence intervals and measurement uncertainties essential for robust mechanical design and accurate numerical simulation. This method fosters a more accurate investigation of material behavior, thereby directly linking experimental findings with the demands of advanced engineering applications.

## 2. METHODOLOGY

### 2.1 Properties of Material and Preparation

The material composition of the AA6061-T6 is shown in the Table 1. It was produced through the technological production scheme, see Figure 1.

TABLE I. AA6061-T6 MATERIAL COMPOSITION

Elements	Amount
Aluminum (Al)	97.29%
Zinc (Zi)	0.05%
Silicon (Si)	0.65%
Cooper (Cu)	0.15%
Chromium (Cr)	0.06%
Magnesium (Mg)	0.92%
Manganese (Mn)	0.05%
Titanium (Ti)	0.02%
Others (%)	0.81%

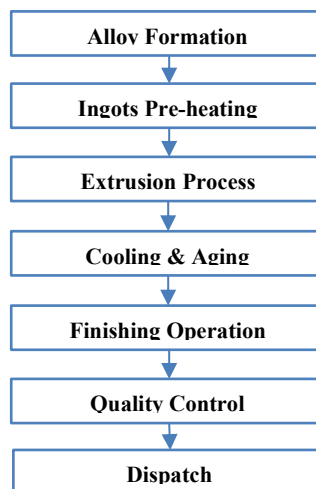


Fig. 1. Scheme of the technological production at Everest ltd [3].

The material used in this study is commercially produced AA6061-T6, supplied in the form of flat stock. Furthermore, rectangular tensile samples of type AA6061 have been machined by using the ASTM E8/E8M standard and a CNC machine to ensure the accuracy of the geometrical dimensions and repeatability [11]. Five samples have been chosen from the same material batch, all of which share with similar chemical composition. In the Table 2 and Figure 2 are shown the rectangular tensile testing samples along associated with their measured dimensions.

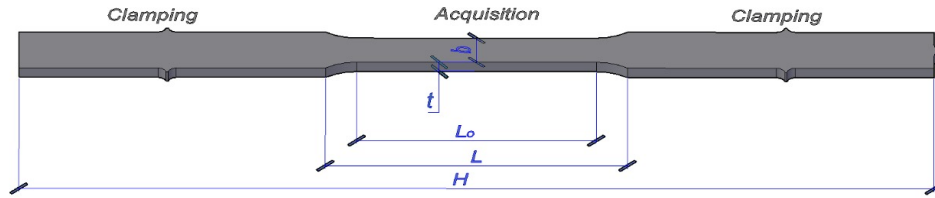


Fig. 2. Design of the tensile sample for AA6061-T6

TABLE II. GEOMETRICAL PARAMETERS AND CORRESPONDING TENSILE PROPERTIES OF THE TESTED SPECIMENS

Sample No.	b (mm)	t (mm)	S <sub>0</sub> (mm <sup>2</sup> )	L <sub>0</sub> (mm)	L (mm)	F (N)	R <sub>m</sub> (N/mm <sup>2</sup> )	A (%)
1	2.65	12.66	33.55	80.04	91.16	10379.364	309.37	13.89%
2	2.68	12.54	33.6	80.03	91.03	10395.672	309.40	13.74%
3	2.66	12.61	33.54	80.02	91.11	10376.605	309.38	13.86%
4	2.67	12.56	33.54	80.04	91.07	10374.593	309.32	13.78%
5	2.65	12.65	33.51	80.02	91.14	10365.983	309.34	13.90%

Were:

$b$  - width of specimen

$t$  - thickness

$S_0$  - original cross-sectional area

$L_0$  - original gauge length

$L$  - length of displacement measurement section

$F_{\max}$  - maximum applied force

$A$  - elongation

$R_m$  - tensile strength

$H$  - sample length which corresponds to 250 mm

## 2.2 Procedure of the tensile testing

The AA6061-T6 tensile testing samples were carried out at ambient temperature by using the standard ISO 6892-1:2020 [20]. Figure 3 presents the configuration of the calibrated uniaxial tensile strength machine, model EUROTTEST-100. An extensometer was attached to the specimen to record the axial strain. The displacement and force were recorded in continuously manner until the sample fractured.

Furthermore, the equation (1) was used to determine the tensile strength of the AA6061-T6.

$$R_m = \frac{F_{\max}}{S_0} = \frac{F_{\max}}{b \cdot t} \quad (1)$$

Elongation ( $A$ ), a crucial measure of mechanical properties such as safety, ductility, and quality has been evaluated through the equation (2).

$$A = \frac{L - L_0}{L_0} \cdot 100\% \quad (2)$$



Fig. 3. Tensile testing arrangement for the produced AA6061-T6

### 3. QUALITY ASSURANCE

Quality assurance is crucial for guaranteeing where the fabricated product adheres to the necessary specifications. Based on it, quality control has been implemented in the following manner:

- Investigation of the micrograph
- Tensile testing
- Assessment of measurement uncertainty

#### 3.1 Investigation of the Micrograph

The ingots has a sample diameter of 178 mm that will be used for fabricated AA6061-T6 was chosen and examined, as illustrated in Figure 4. The micrographic analysis was performed in accordance with the ASTM E407-07, ASTM E112-13, and ASTM E3-11 standards. [21-23]. The macrographic examination was conducted using the microscope model LEICA Z16APOA [24].

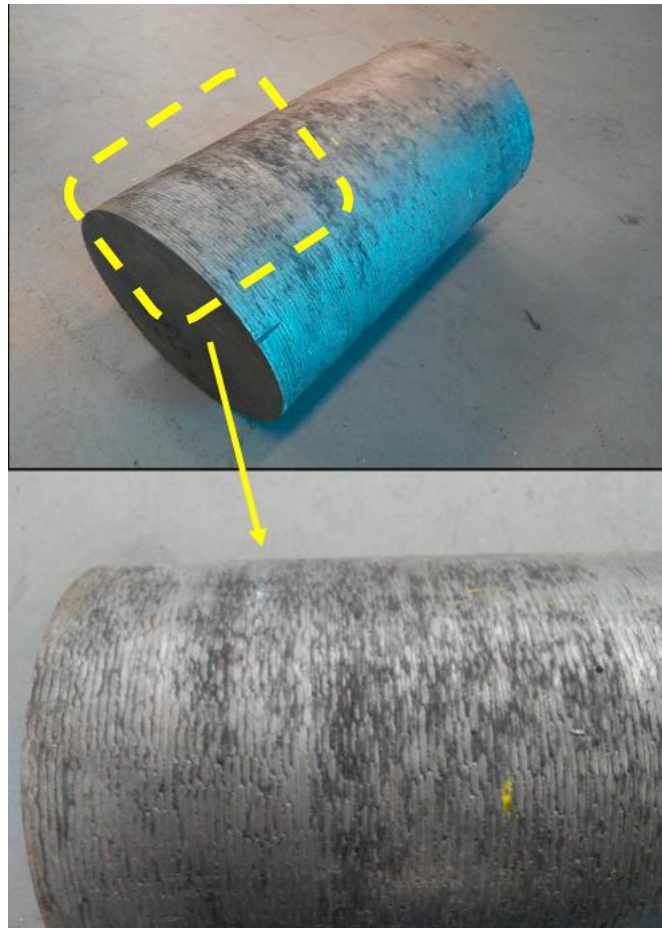
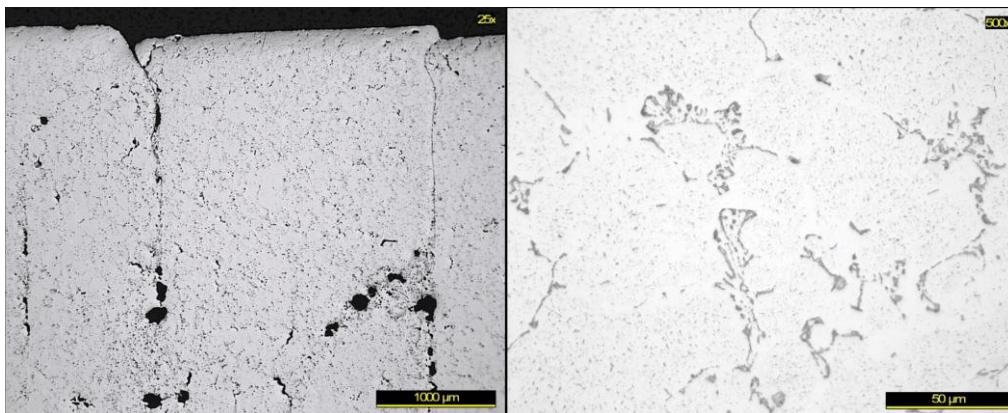


**Fig. 4.** Selection of the AA6061 sample from the ingot material

Furthermore, the ingots has been selected for AA6061-T6 was used for micrograph analysis, and is illustrated in the Figure 5.



(a)

(b)

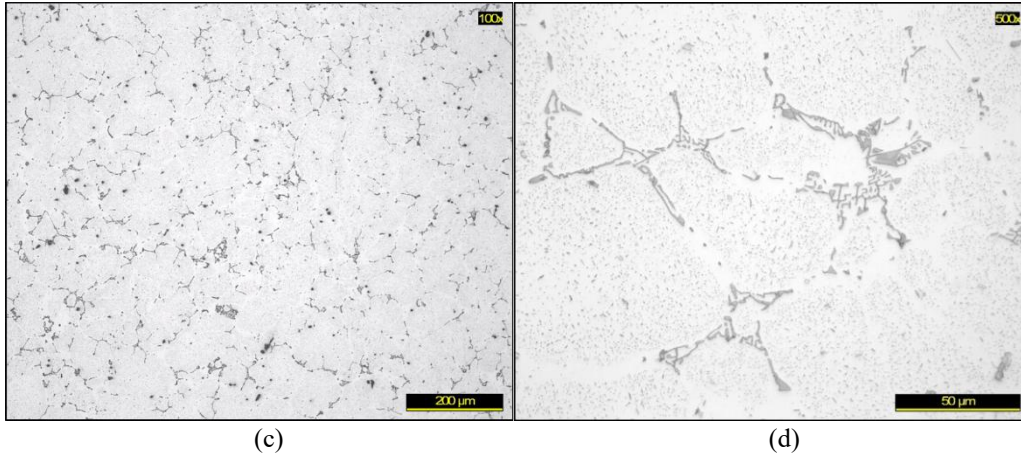


Fig. 5. Microstructural analysis of AA6061 ingots: (a)- longitudinal section at the outer surface; (b)- transverse section at the outer surface; (c)- longitudinal section at mid-radius; (d)-transverse section at the center; (d) - Grain size

Figure 5a depicts the surface discontinuities in the longitudinal section indicate segregations accompanied with porosity, shrinkage micro-cavities, and solidification folds, extending to depths of 3–5 mm. Figure 5b shows an  $\alpha$ -aluminum matrix with complex interdendritic intermetallics and finely distributed phases. Figures 5c and 5d show a similar microstructure consisting of an  $\alpha$ -aluminum matrix with complex interdendritic intermetallic constituents and uniformly distributed particles.

Figure 5d depicts the image of the grain size and it has been used to support the mechanical findings. Based on it, we have used at least 5 straight test lines which are randomly oriented to avoid image edges as can be seen in Figure 6. Each straight lines correspond to approximately 200  $\mu\text{m}$  long and the total test line length was  $L_T \approx 1000 \mu\text{m}$ . In visual inspection, each 200  $\mu\text{m}$  line crosses about 5–6 grain boundaries and for 5 lines the total intercepts  $N$  correspond approximately to 27 until 30. The mean lineal intercept length has been calculated by using equation (3):

$$\bar{l} = \frac{L_T}{N} \tag{3}$$

By using a mid-range count where  $N = 28$  and  $L_T = 1000 \mu\text{m}$  the mean lineal intercept corresponds to 35.7  $\mu\text{m}$ . To convert in ASTM grain size number, we have used the equation (4) with  $\bar{l} = 35.7 \mu\text{m}$  [22].

$$G = -6.6439 \log_{10}(\bar{l}) - 3.288 \tag{4}$$

Based on the above equation the grain size corresponds to  $G = 6.7$ .

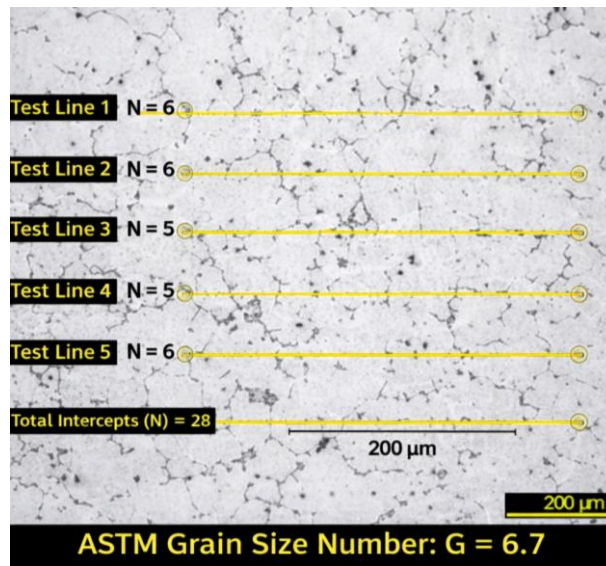


Fig. 6. Grain size for AA6061

### 3.2 Results of Tensile Testing

Tensile testing results are shown in Table 2 for five chosen samples. Additionally, Figure 7 illustrates the diagram of selected sample 2, and corresponds in our case to the highest tensile strength.

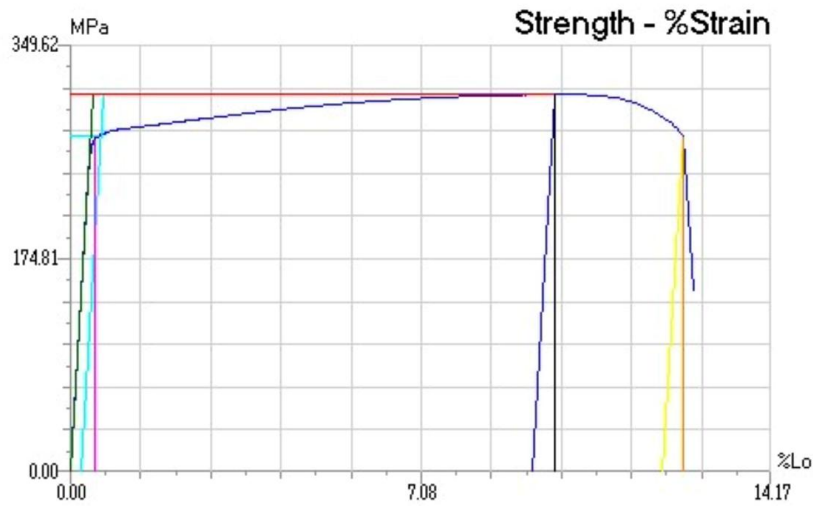


Fig. 7. Diagram of the AA6061 tensile test results.

Furthermore, the outcomes of the chosen sample 2 were displayed in Table 3 and were contrasted with the established standards.

Table III. AA6061-T6 TENSILE TESTING RESULTS

Requirements / Results	Rm (N/mm <sup>2</sup> )	A (%)
Standard ISO 6892-1 [25]	≥300	≥12
Results	309.4	13.74

The assessment of measurement uncertainty is playing important role for ensuring the quality of the fabricated AA6061-T6. The Guide to the Expression of Uncertainty in Measurement (GUM) has been used to make the assessment of measurement uncertainty [25]. The model for measuring uniaxial tensile strength, denoted as  $y$ , was employed to evaluate the measurement uncertainty, with particular attention given to the uncertainty sources outlined in equation (5).

$$y = x + K_1 + K_2 + K_3 + K_4 + K_5 + K_6 \tag{5}$$

Where,  $x$  denotes measured tensile strength value,  $K_1$  indicates the adjustment based on the width reading,  $K_2$  reflects the adjustment based on the thickness reading,  $K_3$  represents the adjustment based on the force reading,  $K_4$  illustrates the adjustment resulting from the calibration of the uniaxial tensile strength device,  $K_5$  signifies the adjustment due to the resolution of the width, and  $K_6$  pertains to the adjustment due to the resolution of the thickness.

The principle of uncertainty propagation has been utilized to assess the overall uncertainty by employing equation (6). The combined uncertainty has been determined by the contributions from the various uncertainty sources.

$$u_c(y) = \sqrt{u_{K_1}^2 \cdot c_1^2 + u_{K_2}^2 \cdot c_2^2 + u_{K_3}^2 \cdot c_3^2 + u_{K_4}^2 \cdot c_4^2 + u_{K_5}^2 \cdot c_5^2 + u_{K_6}^2 \cdot c_6^2} \tag{6}$$

Where:

- $u_{K_1}$  - standard uncertainty of the width measurement,
- $u_{K_2}$  - standard uncertainty of the thickness measurement,
- $u_{K_3}$  - standard uncertainty related to the applied load reading
- $u_{K_4}$  - calibration uncertainty from the tensile strength device
- $u_{K_5}$  - uncertainty associated with caliper resolution, width
- $u_{K_6}$  - uncertainty associated with caliper resolution, thickness.

Based on the repeatability measurements, statistical analysis was employed to determine the standard uncertainties of the width  $u_{\{K1\}}$  and thickness  $u_{\{K2\}}$  using Equations (7) and (8), respectively.

$$u_{k1} = \sqrt{u_w^2 + u_{\Delta w}^2} \quad (7)$$

$$u_{k2} = \sqrt{u_t^2 + u_{\Delta t}^2} \quad (8)$$

Where  $u_t$  and  $u_w$  represent the standard uncertainties associated with the measurements respectively of thickness and width. Additionally,  $\Delta w$  and  $\Delta t$  denote the relative uncertainties for length and width, which correspond to the values  $\Delta t = \Delta w = 0.05$  mm.

The standard deviation of the readings in the applied loads has been determined by using the standard uncertainty associated via equation (9).

$$u_{k3} = \sqrt{\frac{1}{n-1} \sum_{i=1}^n (x_i - x_m)^2} \quad (9)$$

Where:

$n$  - applied load measurement values, complete set

$x_i$  - individual measurement value

$x_m$  - mean values of the individual measurements.

Equation (10) has been used to determine the calibration uncertainty for the tensile strength.

$$u_{k4} = \frac{p \cdot F_m}{\sqrt{3}} \quad (10)$$

Where:

$p$  - relative accuracy from the load cell with a value 0.005

$F_m$  - average measured force value.

The uncertainty arising from the caliper resolution for both width and thickness was evaluated through equation (11).

$$u_{k5} = u_{k6} = \frac{a}{\sqrt{3}} \quad (11)$$

Where  $a$  denotes the caliper resolution with a value 0.01 mm.

Moreover, the sensitivity coefficients for force, width, and thickness were determined by taking the partial derivative of the tensile strength as outlined in equation (1), and has been expressed through equations (12) to (14).

$$C_1 = C_4 = \frac{\partial R_m}{\partial F} = \frac{1}{b \cdot t} \quad (12)$$

$$C_2 = C_5 = \frac{\partial R_m}{\partial b} = \frac{F_m}{b^2 \cdot t} \quad (13)$$

$$C_3 = C_6 = \frac{\partial R_m}{\partial F} = \frac{F_m}{b \cdot t^2} \quad (14)$$

Furthermore, we have used the equation (15) to evaluate the expanded uncertainty  $U$ .

$$U = k \cdot u_c(y) \quad (15)$$

Where,  $k$  denotes the coverage factor with value 2, corresponding to a 95% confidence level.

The budget of uncertainty to determine the mechanical strength of AA6061 sample is presented below in the Table 4.

The obtained value of the tensile strength was  $309.4 \pm 4.0$  N/mm<sup>2</sup> for  $k = 2$ , which shows a strong correlation with the standard requirements for the AA6061 alloy. Additionally, we have used the equation (16) for evaluated the relative uncertainty.

$$U_r = \frac{U}{R_m} \cdot 100\% \quad (16)$$

The relative uncertainty was calculated as 1.3%, confirming the reliability of the experimental methodology and the suitability of the applied uncertainty assessment. Therefore, the results are accurate and appropriate for quality control and the characterization of mechanical properties.

**Table IV.** BUDGET OF UNCERTAINTY FOR THE FABRICATED AA6061-T6 SAMPLE

Sources of Uncertainty	Standard Uncertainty, $u_i$	Probability Distribution	Sensitivity Coefficient, $C_i$	Uncertainty (N/mm <sup>2</sup> )
Reading of the thickness	0.026 (mm)	Normal	65.6 (N/mm <sup>3</sup> )	1.71
Reading of the width	0.006 (mm)	Normal	116.3 (N/mm <sup>3</sup> )	0.69
Reading of the applied load	5.426 (N)	Normal	0.0029 (1/mm <sup>2</sup> )	0.015
Caliper resolution, width	0.0058 (mm)	Rectangular	116.3 (N/mm <sup>3</sup> )	0.67
Caliper resolution, thickness	0.0058 (mm)	Rectangular	65.6 (N/mm <sup>3</sup> )	0.38
Calibration, Tensile Strength Device	29.9 (N)	Rectangular	0.0029 (1/mm <sup>2</sup> )	0.087
Combined Uncertainty, $k = 1$				2
Expanded Uncertainty, $k = 2$				4

#### 4. SUMMARY AND CONCLUSION

This paper presents a novelty methodology that combines the experimental mechanical evaluation of a fabricated AA6061-T6 with a structured process to assess the measurement uncertainty. Comprehensive quality assessment procedures were conducted, yielding very good results in tensile testing, microstructural analysis, and uncertainty evaluation, all in accordance with relevant international standards. Due to our findings the following conclusions have been drawn:

- The measured tensile strength of the produced AA6061 alloy specimen was  $309.4 \pm 4.0$  N/mm<sup>2</sup> ( $k = 2$ ), which lies within the standard range for AA6061 alloys. This confirms that the material meets the required mechanical property specifications. The low relative expanded uncertainty of 1.3% reflects high measurement accuracy and strong experimental consistency.
- The small magnitude of the expanded uncertainty (1.3%) demonstrates precise measurements and reliable test repeatability.
- The budget of the uncertainty analysis has shown that sample thickness measurement contributes the most to the overall uncertainty, while the effect from force measurement remains minor consistent with expectations for flat specimen tensile tests.
- The uncertainty assessment method applied in this work adheres to ISO/IEC Guide 98-3 (GUM), proving it to be a dependable tool for quality assurance, mechanical testing, and conformity evaluations of aluminum alloys.
- The measurement test results verify that the material type AA6061-T6 exhibits stable with very good mechanical behavior.

The combined experimental and analytical methodology provides accurate, repeatable outcomes, making it well-suited for both engineering applications and research studies.

#### Conflicts of Interest

The authors declare no conflict of interest.

#### Funding

This research received no external funding.

#### Acknowledgment

Non.

#### References

- [1] L. Wang, Z. Zhang, Y. Luo, Y. Xiao, F. Tan, and K. Liu, "Understanding the influencing mechanism of CNTs on the microstructures and wear characterization of semi-solid stir casting Al-Cu-Mg-Si alloys," *Metals*, vol. 12, p. 2171, 2022.

- [2] W. Shi, L. Chen, B. He, B. Lu, and J. Yang, "Effect of Al-5Ti-2B on the microstructure and mechanical properties of recycled Al-7Si-0.3Mg-1Fe alloy," *Crystals*, vol. 15, no. 7, p. 584, 2025.
- [3] K. Dhoska, I. Markja, E. Bebi, A. Sulejmani, O. Koça, E. Sita, and A. Pramono, "Manufacturing process of the aluminum alloy AA6063 for engineering applications," *Journal of Integrated Engineering and Applied Sciences*, vol. 1, no. 1, pp. 1–13, 2023.
- [4] H. Khalilpoor, D. Larouche, X. G. Chen, A. Phillion, and J. Colbert, "Investigation of the hydrostatic pressure effect on the formation of hot tearing in the AA6111 alloy during direct chill casting of rectangular ingots," *Applied Mechanics*, vol. 6, no. 3, p. 53, 2025.
- [5] A. Pramono, O. Nežerenko, M. Fitrullah, and Suryana, "Microstructural evolution and mechanical properties enhancement of Ti/SiC metal matrix composites," *Journal of Transactions in Systems Engineering*, vol. 2, no. 3, pp. 295–305, 2024.
- [6] S. Duan, Y. Lu, A. Li, M. Tang, W. Chen, C. Huang, J. Du, Y. Xu, and Y. Yan, "Synergistic effect of Cu addition and pre-straining on the natural aging and artificial age-hardening behavior of AA6111 alloy," *Materials*, vol. 18, no. 7, p. 1635, 2025.
- [7] G. E. Totten and D. S. MacKenzie, *Handbook of Aluminum: Volume 1: Physical Metallurgy and Processes*. New York, NY, USA: Marcel Dekker, 2003.
- [8] I. J. Polmear, *Light Alloys: From Traditional Alloys to Nanocrystals*, 4th ed. Oxford, U.K.: Butterworth-Heinemann, 2006.
- [9] Z. Chen, C. Li, F. Li, and C. Li, "Enhancing the mechanical properties of 6061 aluminum alloy through the synergistic effects of twins, stacking faults, nanograins and lattice distortions," *Journal of Materials Research and Technology*, vol. 35, pp. 6650–6658, 2025.
- [10] P. N. Rao, D. Singh, and R. Jayaganthan, "Mechanical properties and microstructural evolution of Al 6061 alloy processed by multidirectional forging at liquid nitrogen temperature," *Materials & Design*, vol. 56, pp. 97–104, 2014.
- [11] ASTM E8/E8M-24, "Standard test methods for tension testing of metallic materials," ASTM International, West Conshohocken, PA, USA, 2024.
- [12] H. B. Motra, A. Dimmig-Osburg, and J. Hildebrand, "Evaluation of experimental measurement uncertainty in engineering properties of PCC samples," *Journal of Civil Engineering Research*, vol. 3, no. 3, pp. 104–113, 2013.
- [13] D. Brizard, S. Ronel, and E. Jacquelin, "Estimating measurement uncertainty on stress-strain curves from SHPB," *Experimental Mechanics*, vol. 57, no. 5, pp. 735–742, 2017.
- [14] S. Salicone, "New frontiers in measurement uncertainty," *Metrology*, vol. 2, no. 4, pp. 495–498, 2022.
- [15] K. Dhoska, S. Tola, A. Pramono, and I. Vozga, "Evaluation of measurement uncertainty for the determination of the mechanical resistance of the brick samples by using uniaxial compressive strength test," *International Journal of Metrology and Quality Engineering*, vol. 9, no. 12, pp. 1–5, 2018.
- [16] D. Kuhinek, I. Zorić, and P. Hržejnjak, "Measurement uncertainty in testing of uniaxial compressive strength and deformability of rock samples," *Measurement Science Review*, vol. 11, no. 4, 2011.
- [17] B. Kommey, S. Kyei Agyemang, J. Owusu Yeboah, H. Tunteiya Hardy, and S. Asuo-Darko, "A comprehensive study of causal factors and their effects on the human body for the design of a smart bed sore prevention system," *International Journal of Innovative Technology and Interdisciplinary Sciences*, vol. 6, no. 3, pp. 1220–1235, 2023.
- [18] O. Rodriguez-Alabanda, M. A. Narvaez, G. Guerrero-Vaca, and P. E. Romero, "Manufacturing of non-stick molds from pre-painted aluminum sheets via single point incremental forming," *Applied Sciences*, vol. 8, no. 6, p. 1002, 2018.
- [19] S. Khosal, D. De, D. Kar Ray, and T. Roy, "Condition monitoring of fixed and dual axis tracker using curve fitting technique," *International Journal of Innovative Technology and Interdisciplinary Sciences*, vol. 6, no. 4, pp. 1264–1272, 2023.

- [20] UNI EN ISO 6892-1:2020, “Metallic materials—Tensile testing—Part 1: Method of test at room temperature,” International Organization for Standardization, 2020.
- [21] ASTM E3-11, “Standard guide for preparation of metallographic specimens,” ASTM International, West Conshohocken, PA, USA, 2017.
- [22] ASTM E112-13, “Standard test methods for determining average grain size,” ASTM International, West Conshohocken, PA, USA, 2021.
- [23] ASTM E407-07, “Standard practice for microetching metals and alloys,” ASTM International, West Conshohocken, PA, USA, 2015.
- [24] Leica Z16 APO Stereo Motorized Microscope, available: <https://coastalmicroscopes.com/products/leica-z16-apo-stereo-motorized-microscope-bm-1890> (accessed Oct. 12, 2025).
- [25] ISO/IEC Guide 98-3:2008, “Uncertainty of measurement—Part 3: Guide to the expression of uncertainty in measurement (GUM),” ISO, Geneva, Switzerland, 2008.